DEHYDROXYLATION AND TRANSFORMATIONS OF THE 2:1 PHYLLOSILICATE PYROPHYLLITE AT ELEVATED TEMPERATURES: AN INFRARED SPECTROSCOPIC STUDY

Ling Wang[1,2,*], Ming Zhang[2], Simon A. T. Redfern[2] and Zhenyu Zhang[3]

[1] Changsha Institute of Geotectonics, Chinese Academy of Sciences, Changsha 410013, P.R. China
[2] Department of Earth Sciences, University of Cambridge, Downing Street, Cambridge CB2 3EQ, UK
[3] Institute of Geology and Geophysics, Chinese Academy of Sciences, Beijing 100029, P. R. China

Abstract—The thermally-induced dehydroxylation and transformations of the 2:1 phyllosilicate pyrophyllite have been studied using infrared spectroscopy in the frequency range $350-11000$ cm^{-1} and the temperature range $200-1500°C$. The dehydroxylation of pyrophyllite to pyrophyllite dehydroxylate occurs between 500 and $900°C$. It is characterized by a decrease in the intensity of the OH signals and phonon bands of pyrophyllite and the eventual disappearance of these features as well as the appearance of extra signals related to pyrophyllite dehydroxylate and an intermediate phase. Our results are consistent with previous observations that the SiO_4 tetrahedral sheet structure still exists in pyrophyllite dehydroxylate, that the Si−O−Al linkages and 2:1 structure remain in the pyrophyllite dehydroxylate, and that AlO_5 trigonal bipyramids form.

Two extra OH bands at 3690 and 3702 cm^{-1} and their overtones at 7208 and 7234 cm^{-1} are observed, for the first time, in samples annealed at the temperature range $550-900°C$. Our results suggest that the formation and dehydroxylation of the extra OH species can be strongly affected by kinetic effects. The experimental evidence shows that the dehydroxylation of pyrophyllite is a two-stage process. The appearance of these additional OH bands is interpreted in terms of an unknown intermediate phase, and may be related to the second endothermic peak observed at high temperatures in DTA experiments. Pyrophyllite dehydroylate decomposes into a Si-rich amorphous phase and mullite in the temperature range $950-1100°C$. Cristobalite is observed in the temperature range $1150-1500°C$.

Key Words—Cristobalite, Dehydroxylation, IR Spectroscopy, Intermediate Phase, Mullite, Pyrophyllite Dehydroxylate, Transformation.

INTRODUCTION

Pyrophyllite, $Al_2Si_4O_{10}(OH)_2$, is a 2:1 aluminosilicate clay. Like muscovite, it has a dioctahedral layered structure in which a sheet of octahedrally coordinated Al ions is sandwiched between two sheets of linked SiO_4 tetrahedra (Bailey, 1966; Rayner and Brown, 1966; Wardle and Brindley, 1972). There are two polytypes of pyrophyllite: two-layered monoclinic ($2M$) and one-layered triclinic ($1Tc$). Mixtures of the two forms ($2M + 1Tc$, or $1Tc + 2M$) are also found in nature (Brindley and Wardle, 1970; Wardle and Brindley, 1972; Eberl, 1979; Lee and Guggenheim, 1981; Wang, 1994; Yang *et al*., 1994). Pyrophyllite has been widely used in industry, especially in the manufacture of ceramics, glass, refractory materials and pressure-transfer media. A deeper understanding of dehydroxylation and transformation of pyrophyllite would be useful for these industrial applications.

The dehydroxylation of pyrophyllite to pyrophyllite dehydroxylate involves the reaction of two OH groups (adjacent to each other on an Al octahedron) with the liberation of water (Fitzgerald *et al*., 1996). Powder X-ray diffraction (XRD) measurements of $1Tc$ pyrophyllite and its dehydroxylate have shown that pyrophyllite dehydroxylate consists of 5-coordinate, distorted, trigonal bipyramidal AlO_5 structural units in the Al oxide layer, sandwiched between two distorted but intact tetrahedral silica layers (Wardle and Brindley, 1971, 1972). ^{29}Si MAS-NMR data have confirmed that pyrophyllite dehydroxylate maintains the 2:1 layer structure (Frost and Barrron, 1984). MAS ^{27}Al NMR studies at a magnetic field strength of 14 T and 16.0 kHz spinning speeds have shown that 6-coordinate Al in pyrophyllite change their structural arrangement to 5-coordinate Al in pyrophyllite dehydroxylate (Fitzgerald *et al*., 1989; 1996). Thermally-induced transformations of pyrophyllite dehydroxylate have been reported. Heller (1962) studied the thermal transfomation of pyrophyllite to mullite in the temperature range $970-1200°C$. Solid-state multinuclear magic-angle spinning (MAS) NMR studies of the thermal transfomations of pyrophyllite, over the temperature range $150-1350°C$ are reported by Fitzgerald *et al*. (1996). High-temperature phases of decomposed pyrophyllite and their evolutionary characteristics were reported by Wang and Zhang (1997a) using powder XRD. However, the behaviors and processes of thermally-induced dehydroxylation and transformation of pyrophyllite remain only partially understood.

We undertook this study to investigate the thermally-induced dehydroxylation of pyrophyllite to pyrophyllite

* E-mail address of corresponding author:
wangling@ms.csig.ac.cn

dehydroxylate and the transformations of pyrophyllite dehydroxylate using IR spectroscopy because it has been widely employed for the study of mineral crystal structures and their behaviors on dehydroxylation and transformation (*e.g.* Bray *et al.*, 1998; Bray and Redfern, 2000). The major advantages of IR spectroscopy are short correlation scale (a few unit-cells), fast response time (~10^{-12} s) and high sensitivity to OH species. Our results provide detailed structural information of the high-temperature behavior of pyrophyllite.

EXPERIMENTAL METHODS

Sample EM08 is a pyrophyllite ($2M + 1Tc$) from the Emei large pyrophyllite deposit, Fuzhou, China. Sample SK06 is a pyrophyllite ($2M$) from the Shankou large pyrophyllite deposit, Qingtian, China. The chemical compositions of the two samples are almost identical to the ideal value of pyrophyllite (Wang, 1994).

Thermal treatments of pyrophyllite samples EM08 and SK06 were carried out between 200 and 1500°C for periods of 15 min, 1 h, and 5 days in a vertical furnace. The furnace was heated to the desired temperature before sample loading. Two Pt-PtRh thermocouples were used in the furnace; one was coupled with a Eurotherm temperature controller, and the second was used to measure the annealing temperature. The instability of the annealing temperature was <5°C. Three types of samples were used for the annealing: small grains (size = 40−60 mesh), powder (size is $\cong 200$ mesh) and thin plates (with a thickness of 0.30 ± 0.02 mm). Fresh gains were annealed thermally at various temperatures for designated periods of time and the samples were measured after quenching. However, the thin plates were annealed for the designated period of time, then after they had been measured at room temperature, they were further annealed at a higher temperature.

The conventional KBr pellet techniques previously reported by Zhang *et al.* (1996) were employed for IR absorption measurements between 350 and 5000 cm^{-1}. The annealed samples were ground with an agate mortar and pestle, and the powdered samples were dried at 110°C for 12 h to remove any possible water adsorbed during grinding. Samples of 3 mg of fine sample powders were thoroughly mixed with 900 mg of dry KBr powder; 200 mg of the sample/matrix mixtures were pressed into disc-shaped pellets of 13 mm diameter at room temperature under vacuum. The thin-section samples were polished before thermal annealing.

A Bruker IFS 66v spectrometer was used for IR measurements at room temperature. A DTGS detector, coupled with a KBr beamsplitter and a Globar source were used to record the powder absorption spectra between 350 and 5000 cm^{-1} (with a instrumental resolution of 2 cm^{-1}). For the measurements of thin plates in the frequency region of 3000−13000 cm^{-1}, a tungsten source, a liquid-nitrogen-cooled MCT detector and a CaF$_2$ beamsplitter were used with an instrumental resolution of 4 cm^{-1}. All the spectra were collected under vacuum. Software OPUS-IR (Bruker) was used for data analysis. Peak positions were determined by the secondary derivative method or fitting measured data to Lorentzian functions. Integrated absorbance was obtained by curve-fitting or simply integrating the measured data with linear base lines.

RESULTS

Infrared spectra of the two natural pyrophylllite samples (EM08 and SK06) are shown in Figure 1a (KBr pellets, 350−4000 cm^{-1}) and Figure 1b (thin plates, 3750−11000 cm^{-1}). The spectra of these two samples are basically identical, although their polytypes are different. Table 1 gives the peak positions of pyrophyllite EM08 in the regions 350−1500 cm^{-1} and 3500−11000 cm^{-1}. Seventeen peaks are observed in the lower frequency region (350−1500 cm^{-1}), consistent with the results reported by Ishii *et al.* (1967), Farmer (1974) and Kloprogge and Frost (1999). The characteristic bands of high intensity in this region are near 482, 539, 1050, 1068 and 1122 cm^{-1}. Another characteristic band occurs at 949 cm^{-1} which was assigned to the in-plane OH libration (Russell *et al.*, 1970). A number of peaks appear between 3500 and 7500 cm^{-1}. Intense IR signals are centered at 3675, 3832, 3844, 4613 and 7176 cm^{-1}. These peaks are due to OH stretching and combinations of OH and vibration phonons. The sharp OH stretching at 3675 cm^{-1} is assigned to the Al$_2$OH stretching mode (interaction between OH and Al) (Farmer, 1974). The band near 7176 cm^{-1} is assigned as the first overtone of the OH-stretching vibration near 3675 cm^{-1}. A very weak band at 10508 cm^{-1} is recorded. It is due to the second overtone of the OH stretching.

Infrared spectra (KBr pellets) of the 40−60 mesh samples annealed in the temperature range 200−1500°C for 1 h are shown in Figure 2a (350−500 cm^{-1}) and Figure 3a (3525−3800 cm^{-1}). The IR spectra (KBr pellets) of the 40−60 mesh samples annealed in temperature range 450−1250°C for 5 d are shown in Figure 2b (350−1500 cm^{-1}) and Figure 3b (3525−3800 cm^{-1}). We shall describe the thermal conversion of pyrophyllite in the temperature range RT−1500°C in four separate primary stages.

First stage – unchanged state of pyrophyllite

The first stage of the thermal conversion of pyrophyllite occurs between room temperature and 450°C based on the spectra given in Figures 2a, 2b, 3a and 3b. Compared with the 350−3800 cm^{-1} spectrum of natural pyrophyllite, the spectra of the samples annealed in the temperature range 200−450°C for 1 h or 5 d show almost no difference in their shape and intensity. It is

Table 1. Characteristic IR peaks of pyrophyllite (EM08) untreated and annealed at 750, 900, 1150 and 1500°C for 1 h.

EM08 (RT) PY	EM08 (750°C) PY	PD	EM08 (900°C) PD	EM08 (1150°C) SA+MU	EM08 (1500°C) CR+MU
Wavenumber: 345−1500 cm^{-1}					
385	358	407	407	467	381
395	395	418	420	526	445
418	418	436	436	732	476
458	458	483	485	823	519
482	483	566	568	901	574
517	519	652	652	1110	617
539	539	737	735	1248	736
575	575	802	801		794
626	626	835	833		884
737	737	865	864		1091
813	814	1033	1033		1168
834	835	1049	1047		1201
854	852	1086	1086		
949	950	1136	1138		
1050		1049			
1068		1069			
1122		1121			
Wavenumber: 3500−11000 cm^{-1}					
3675	3675, 3690*, 3702*				
3832	3832				
3844	3844				
4613	4613				
7176	7176, 7208*, 7234*				
10508	10508				

PY = pyrophyllite; PD = pyrophyllite dehydroxylate; SA = Si-rich amorphous phase; MU = mullite; CR = cristobalite; RT = room temperature
For the sample annealed at 750°C for 1 h, the bands indicated by * are the two extra OH bands and their overtones

obvious that the pyrophyllite is stable and its crystal structure remains basically unchanged in the first stage. It is worth mentioning that the 40−60 mesh samples annealed at 300−450°C for 1 h changed their color from pale yellow-green to gray. Also in this temperature range, the higher the heating temperature is, the grayer the sample becomes. This color change was also observed for the thin-plate samples annealed for 15 min and 1 h.

Second stage – dehydroxylation of pyrophyllite

The thermal dehydroxylation of pyrophyllite occurs in the temperature range 500−900°C depending on the annealing time. The process is characterized by two types of change: (1) a decrease in intensity of OH-absorption bands and other vibrational bands of pyrophyllite (Figures 3a and 3b); and (2) the appearance of extra vibrational bands between 350 and 1500 cm^{-1} (Figures 2a and 2b). For the samples annealed for 1 h, OH bands at 949 and 3675 cm^{-1}, as well as others bands of pyrophyllite, show a systematic decrease in their intensity. This implies a loss of OH content (Figure 4). All the peaks of pyrophyllite have disappeared by 900°C. On the other hand, new peaks of an anhydrous pyrophyllite dehydroxylate phase show a gradual increase in their intensity systematically during the dehydroxylation. Most of the new peaks are first visible at 650°C. At 900°C, the intensity of the new peaks reaches a maximum. It is interesting that four peaks at 418, 482, 834 and 1050 cm^{-1} do not show significant changes in their frequencies at this stage. In fact, these four peaks belong to both pyrophyllite and pyrophyllite dehydroxylate. Thus, the pyrophyllite dehydroxylate has 14 bands in the region 350−1500 cm^{-1} (the peak positions are listed in Table1).

One of the most important observations of this study is that an extra OH band at 3690 cm^{-1} is observed during dehydroxylation of samples EM08 (Figure 3a) and SK06. For the samples annealed for 1 h, the new OH peak at 3690 cm^{-1} is observed at 600°C. As shown in the inset of Figure 4, with increasing temperature, the peak shows an increase in its intensity in the temperature range 600−800°C. At 800°C, its relative integrated absorbance (against the total value of OH species before heating) reaches a value of 6% under the condition of our experiment. However, it shows a decrease in its intensity at 850°C and has disappeared at 900°C.

The dehydroxylation is also characterized by the spectral changes in the OH overtones. As described earlier, the IR feature near 7176 cm^{-1} is due to the first
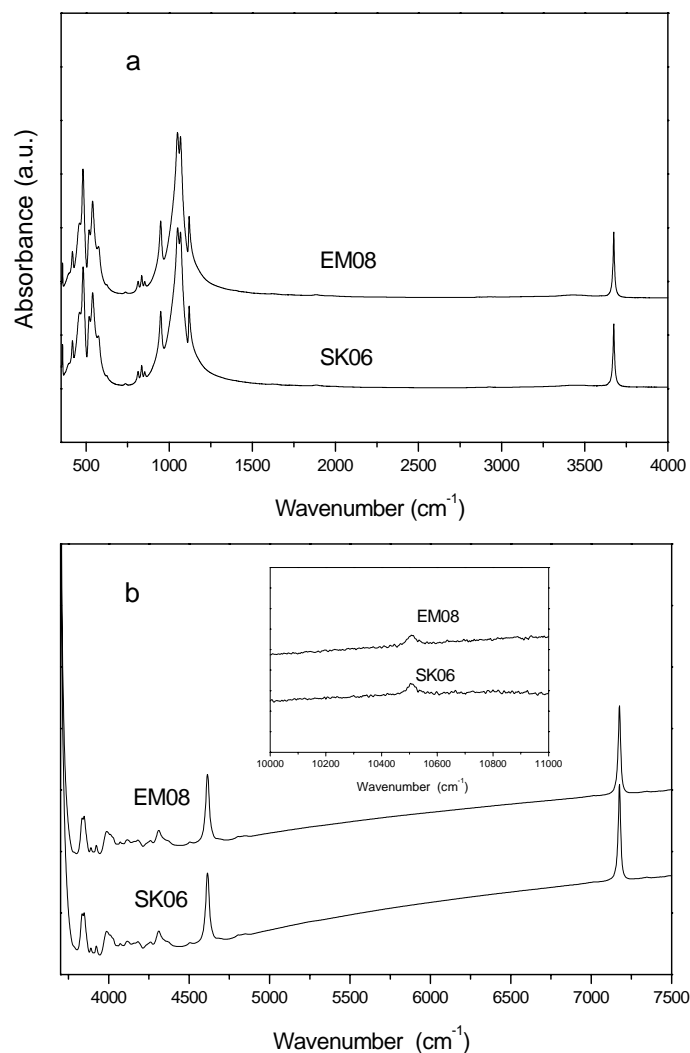
Figure 1. Infrared spectra of the natural pyrophyllites: (a) powder samples (KBr pellets) in the region 350−4000 cm^{-1}; (b) thin-plate samples (0.30 ± 0.02 mm) in the region 3750−11000 cm^{-1}. EM08 = pyrophyllite (2M + 1Tc) from Emei, Fuzhou, China; SK06 = pyrophyllite (2M) from Shankou, Qingtian, China.

overtone of the OH stretching near 3675 cm^{-1}. The temperature evolution of the overtone has been investigated by measuring thin-plate samples, because it is difficult to detect the overtone with IR powder absorption measurements. Although the remaining OH contents in the sample may be affected by sample thickness, the fundamental mechanism of dehydroxylation should not be dramatically altered by the fact that we used thin plates. The thin-plate samples EM08 and SK06 were stepwise annealed at various temperatures for different periods of time, and IR spectra were recorded at room temperature. Annealing times of 15 min (Figure 5a) and 1 h (Figure 5b) were used. As shown in Figures 5a, 5b and 6, for the samples heated for 15 min and 1 h, the OH overtone near 7176 cm^{-1} does not show significant change until 750°C; then it surprisingly shows an increase in its intensity at 800°C and disappears at 900°C.

Furthermore, two extra OH bands at 7208 and 7234 cm^{-1} are observed during the dehydroxylation. The first one is due to the overtone of an OH band at 3690 cm^{-1}. The second would correspond to the overtone of another OH-stretching band, which is not clearly visible in the mid-IR (MIR) region (near 3702 cm^{-1}). As shown in Figure 5a, the peak at 7208 cm^{-1} is weak in the samples annealed at 600°C after heating for 15 min and 750°C after heating for 1 h. With increasing temperature, it shows an increase in its intensity between 600 and 850°C (15 min samples, Figure 5a and the inset of Figure 6) or between 750 and 800°C for the samples annealed for 1 h (Figure 5b). It then disappears at 900°C in both the sample annealed for 15 min and for 1 h. By contrast, the new peak at 7234 cm^{-1} is visible at 800°C (1 h) and in 800−850°C (15 min). It also disappears at 900°C (for both the 15 min and 1 h samples). It could be that the two new peaks exist in the lower temperature
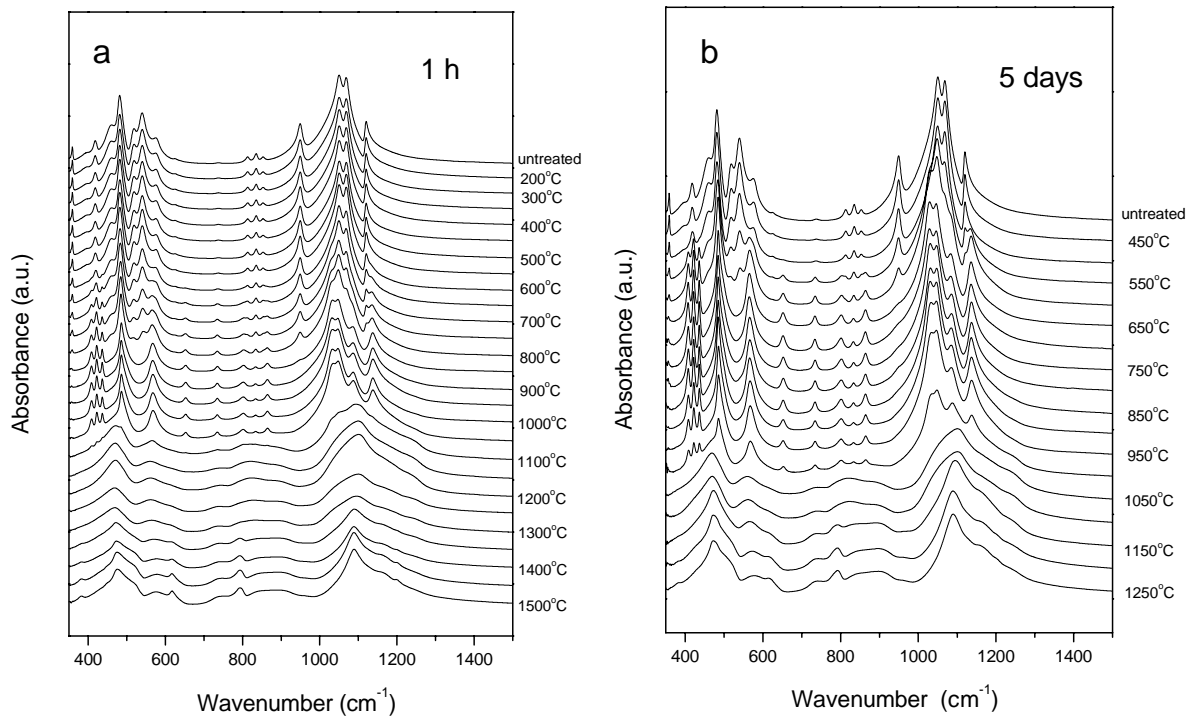
Figure 2. Infrared spectra (KBr pellets) in the region 350–1500 cm^{-1} of pyrophyllite EM08 samples (40–60 mesh) annealed in temperature range: (a) 200–1500°C for 1 h; (b) 450–1250°C for 5 d.
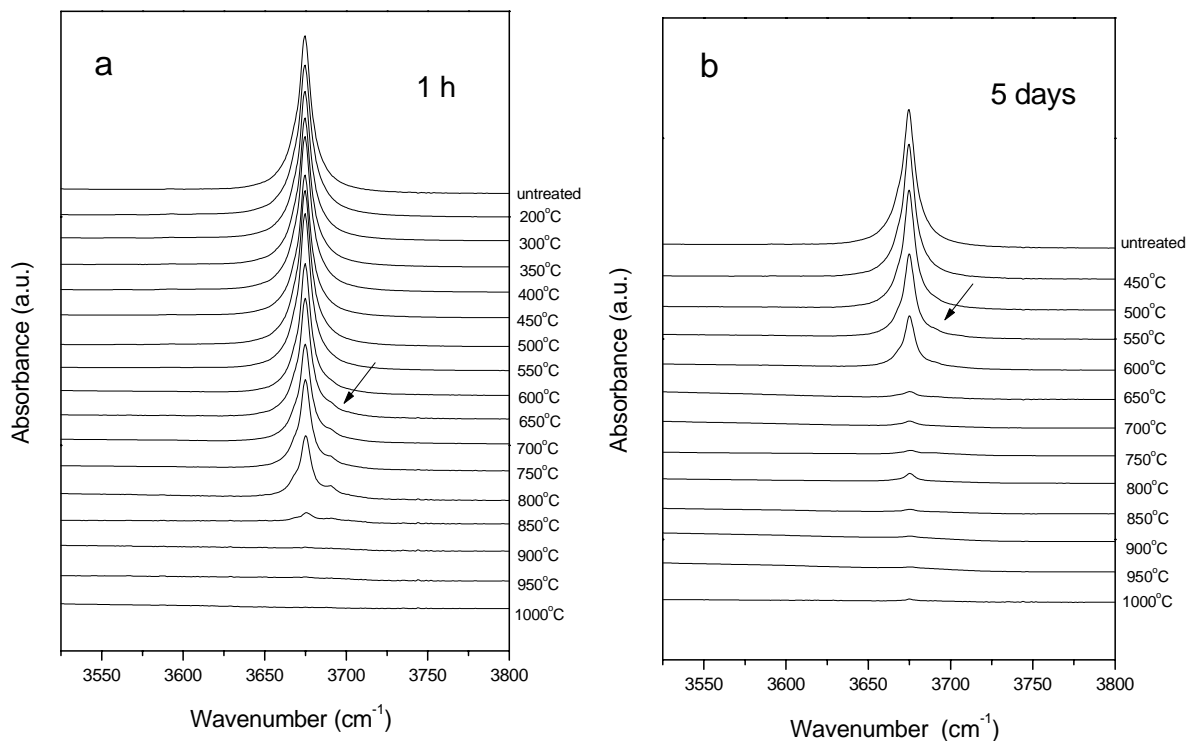

Figure 3. Infrared spectra (KBr pellets) in the region 3525–3800 cm^{-1} of pyrophyllite EM08 samples (40–60 mesh) annealed in temperature range: (a) 200–1000°C for 1 h; (b) 450–1000°C for 5 d. The arrows indicate the extra peak at 3690 cm^{-1}.
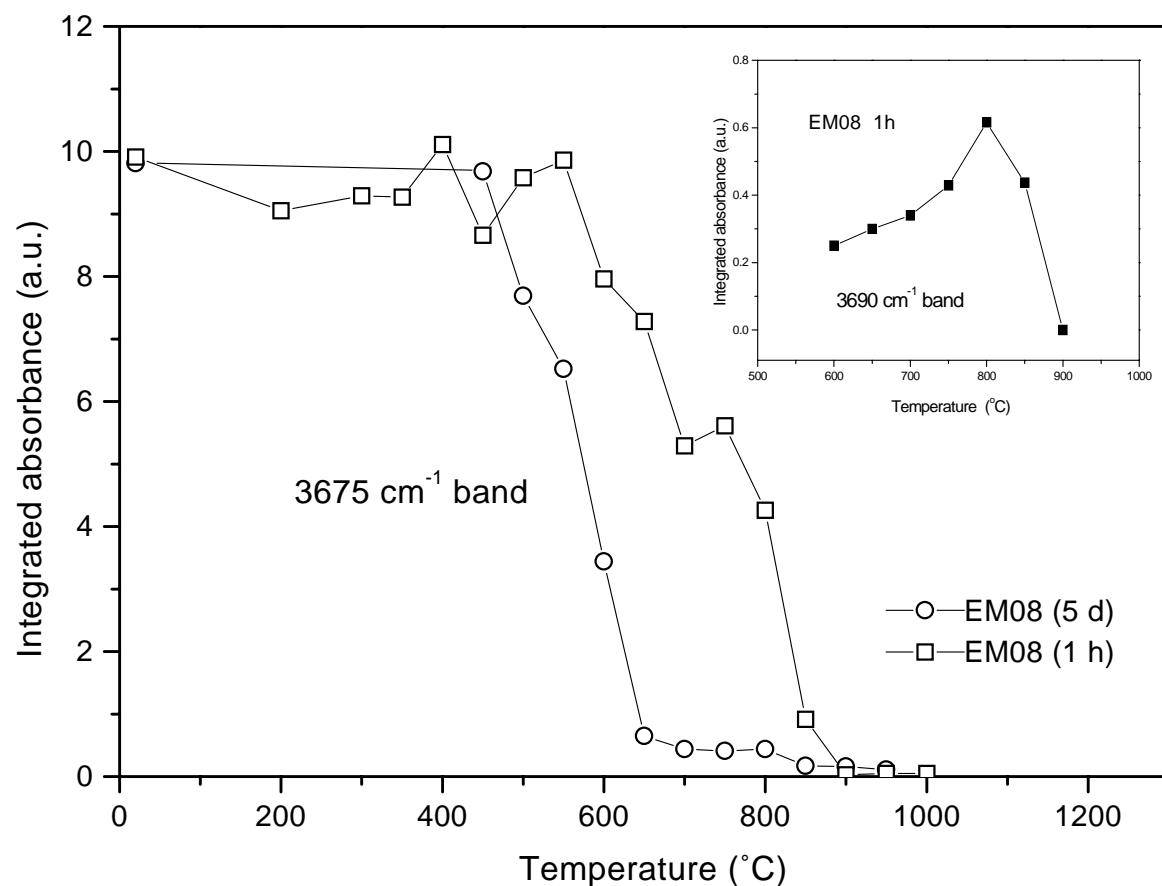
Figure 4. Temperature dependence of integrated absorbance of samples EM08; the OH-stretching bands near 3675 and 3690 cm^{-1}. The integrated absorbance was obtained by integrating the measured data in Figure 3 with linear base lines.

range, but they are so weak that they could not be observed. These results reveal the appearance of two new OH sites during the dehydroxylation process. Similar spectra were recorded for a 2M pyrophyllite sample, SK06.

In order to investigate the thermal stability and the possible activation energy of the additional OH species at 3690 and 3702 cm^{-1}, we checked the effects of annealing time and grain-size on these extra OH signals. The influence of annealing time on the additional OH species can be seen in Figures 2a, 2b, 5a and 5b. The impact of grain-size on the signals is shown in Figure 7. We could not establish the possible temperature at which the dehydroxylation of these new species starts to take place, because of the strong time and grain-size dependence between 600 and 850°C and the limited temperature resolution of our experiment. Our results suggest that the formation and dehydroxylation of the extra OH species can be strongly affected by kinetic effects.

It is worth noting that the samples changed color from gray to white during the second stage of dehydroxylation. For example, for the 40–60 mesh samples heated in the temperature range 500–900°C for

1 h, the higher the heating temperature is, the whiter the sample becomes.

Third stage – decomposition of pyrophyllite dehydroxylate

The third stage, occurring in the temperature range 950–1100°C, is characterized by decomposition of pyrophyllite dehydroxylate. For the samples annealed for 1 h, the decomposition is seen as a decrease in the intensity of the IR signals of pyrophyllite dehydroxylate especially at 1033, 1047, 1086 and 1138 cm^{-1} (Figure 2a,b). This reflects a decrease of the amounts of the pyrophyllite dehydroxylate phase present in the sample with increasing temperature. The peaks of pyrophyllite dehydroxylate disappear after 1050°C (1 h) or 1000°C (5 d). A group of broad peaks at 467, 562, 823, 901, 1110 and 1248 cm^{-1} can clearly be observed from 1100°C (1 h) or 1050°C (5 d). Their broad spectral features imply that the products of decomposed pyrophyllite dehydroxylate are mainly an amorphous phase. In addition, a broad peak at 732 cm^{-1} is detected at 1100°C and it shows an increase in its intensity with increasing temperature. This peak can be assigned as a characteristic signal of mullite (van der
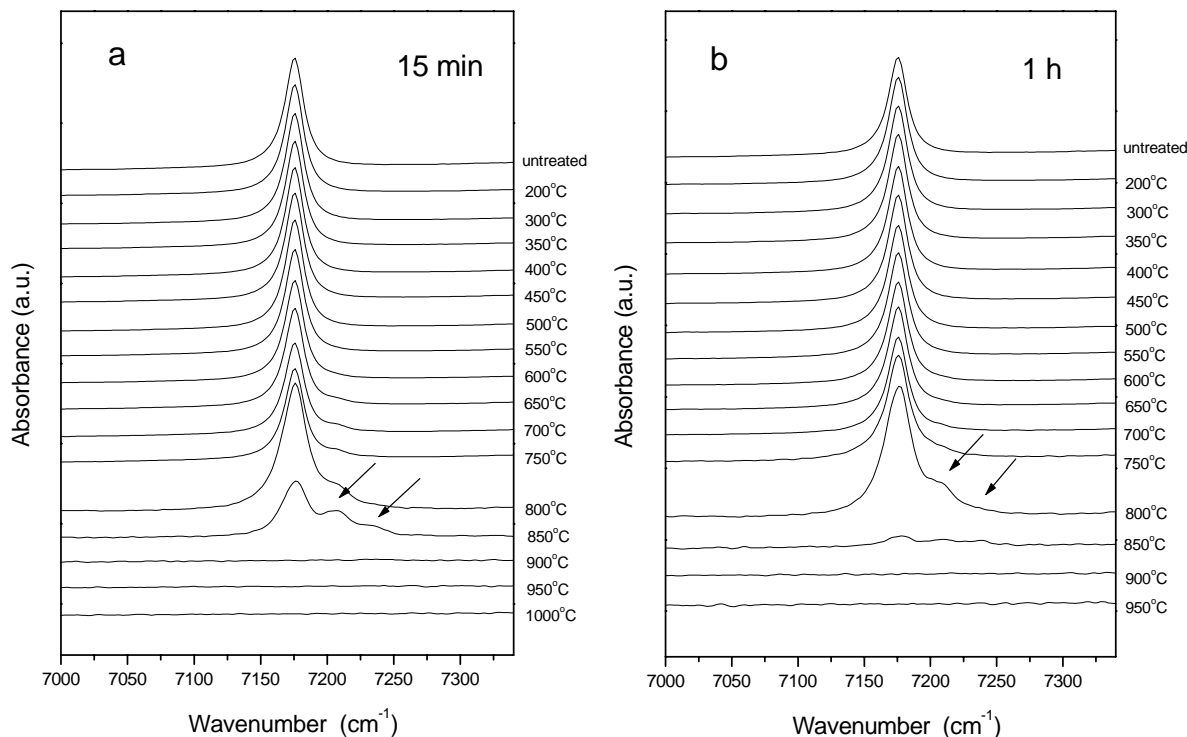
Figure 5. Infrared spectra in the region $7000-7340$ cm^{-1} of the thin-plate pyrophyllite EM08 samples stepwise annealed: (a) $200-1000°C$ for 15 min, 0.32 mm; (b) $200-950°C$ for 1 h, 0.32 mm. The arrows indicate the extra peaks at 7208 and 7234 cm^{-1}.

Marel and Beutelspacher, 1976). Its appearance implies the occurrence of mullite. Its peak is broad and weak too, indicating that the mullite is still poorly ordered and its content is small. Our observation is consistent with the results observed by XRD (Wang and Zhang, 1997a) and solid-state MAS ^{27}Al NMR (Fitzgerald *et al.*, 1996).

Fourth stage − formation of cristobalite

The fourth stage of thermal transformation occurs in the temperature range $1150-1500°C$ based on the spectra given in Figure 2a,b. After annealing at $1150°C$ for 5 d or at $1350°C$ for 1 h, extra peaks at 471, 617, 794 and 1168 cm^{-1} are detected. These are characteristic bands of cristobalite (van der Marel and Beutelspacher, 1976). The results suggest that although cristobalite may form at $1150°C$ (5 days), annealing at this temperature for 1 h may not produce enough cristobalite to be detectable. On increasing the temperature up to $1500°C$ (1 h), these peaks show a further increase in their intensity. At $1500°C$, 12 peaks are visible in range $345-1500$ cm^{-1} (the peak positions are given in Table 1). In comparison with the spectra of synthetic cristobalite (van der Marel and Beutelspacher, 1976), these peaks are mostly assigned to cristobalite and the crystallinity is good.

Since the peaks of mullite are very weak, we only detect its characteristic peaks at 736 and 884 cm^{-1} in samples annealed at $1500°C$ for 1 h or $1250°C$ for 5 d. The content and crystallinity of mullite in the fourth stage appears better than that in the third stage. The

results indicate that the final products in the temperature range $1150-1500°C$ are cristobalite and mullite. These observations are consistent with the XRD results of Wang and Zhang (1997a).

DISCUSSION

Pyrophyllite dehydroxylate structure

As shown in Table 1, pyrophyllite dehydroxylate has 14 absorption bands in the region $345-1500$ cm^{-1}. The sharpness of the absorption bands of the dehydroxylate reflects that it has a well-ordered structure. The changes observed are due to the structural reorganization from pyrophyllite to pyrophyllite dehydroxylate. The band of pyrophyllite at 482 cm^{-1} was ascribed to Si−O vibration (Stubican and Roy, 1961) or Si−O bending vibration (Wen *et al.*, 1988). Wen *et al.* (1988) ascribed the bands of pyrophylllite at 1050, 1068 and 1120 cm^{-1} to Si−O stretching modes. Comparing the spectrum of pyrophyllite dehydroxylate and pyrophyllite, there are only small frequency shifts (Table 1). These changes together with XRD results indicate that the SiO$_4$ tetrahedral sheet structure still exists in the pyrophyllite dehydroxylate, but its structure is distorted or changed. In fact, according to the solid-state ^{29}Si NMR results (Frost and Barron, 1984), significant changes in the average Si−O−Si angle do occur on dehydroxylation. It increases from $132.2°$ to $137.3°$, and the Si−Si interatomic separation increases from 2.98 to 3.03 Å.
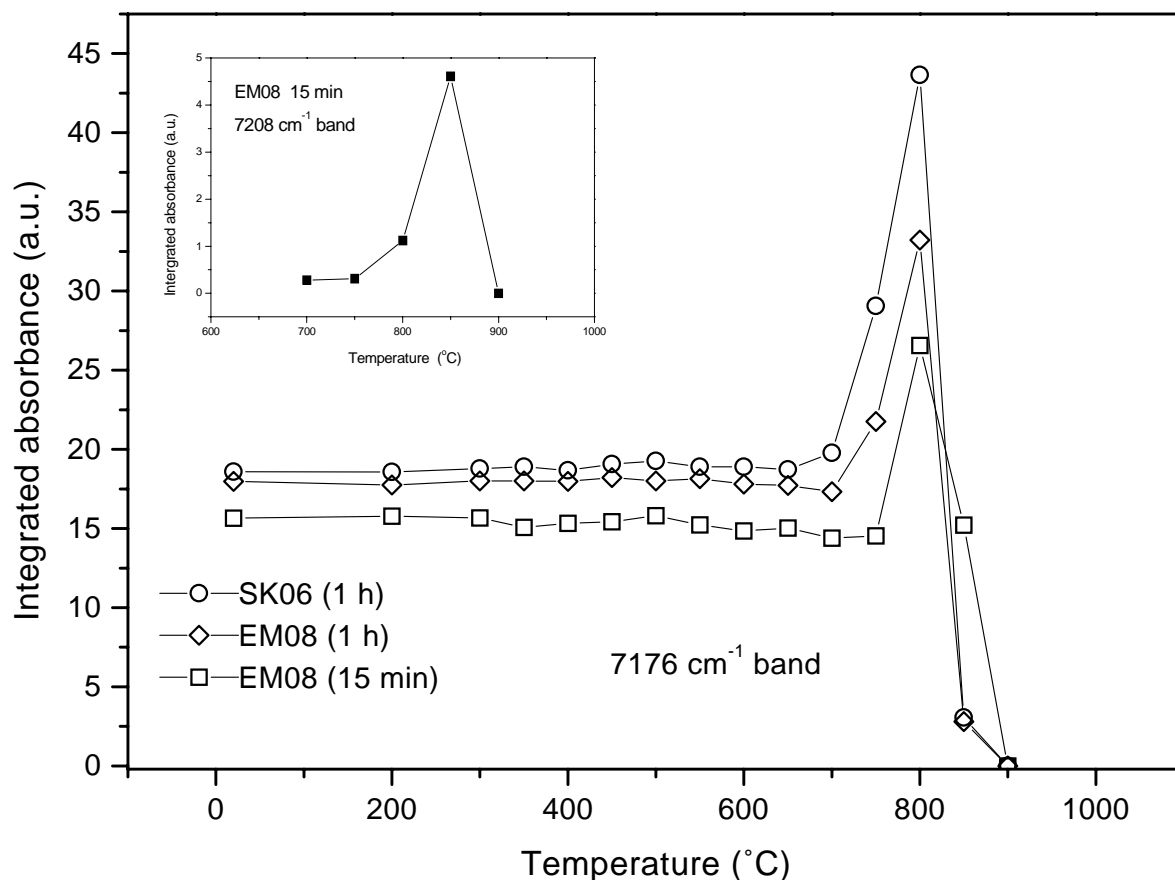
Figure 6. Temperature dependence of integrated absorbance of samples EM08 and SK06; the OH-overtone bands near 7176 and 7208 cm^{-1}. The integrated absorbance was obtained by fitting the measured data in Figure 5 to Lorentzian functions.

The bands of pyrophyllite at 539 and 575 cm^{-1} are ascribed to Si−O−Al^{VI} vibrations by Stubican and Roy (1961) and Wen *et al*. (1988). Pyrophyllite dehydroxylate shows only one sharp band at 568 cm^{-1} in the frequency region. This band can be assigned to a Si−O−Al vibration (Stubican and Roy, 1961), and its occurrence indicates that the Si−O−Al linkages remain. Its frequency change implies a small change in Si−O−Al bond lengths. Our observations are related to the 2:1 layer structure in pyrophyllite dehydroxylate reported by XRD (Wardle and Brindley, 1972; Wang and Zhang, 1997a) and are also consistent with those observed by solid-state ^{27}Al and ^{29}Si NMR (Frost and Barron, 1984; Fitzgerald *et al*., 1996).

There are others four new bands at 568, 652, 801 and 864 cm^{-1} in pyrophyllite dehydroxylate. They are probably due to the structural reorganization from the 6-coordinated Al in the octahedral sheet to 5-coordination after dehydroxylation. The crystal structure results of Wardle and Brindley (1972) clearly show that the dehydroxylate structure is derived by loss of one OH group and the H$^+$ associated with the next OH group. The residual oxygen then moves to the same *z* coordinate level as the Al cation plane and positions itself midway between the two closest Al cations and to form

5-coordinate trigonal bipyramids. Most significantly, based on the results of Wardle and Brindley (1972), there are six different O−Al−O angles with six different O−O interatomic distances respectively, in the AlO$_5$ trigonal bipyramid, which could be associated with the new Al−O−(Si) bands in the region 550−900 cm^{-1}.

Process of pyrophyllite dehydroxylation

The appearance of the extra OH species at 3690 and near 3702 cm^{-1}, as well as their overtones at 7208 and 7234 cm^{-1}, indicates new local structural configurations related to these OH species. As these IR signals are absent in untreated pyrophyllite and pyrophyllite dehydroxylate annealed above 900°C, we interpret them as evidence of an unknown intermediate structural state, which has a local environment different to those of pyrophyllite and pyrophyllite dehydroxylate. At this stage we can consider two possible paths, or combinations of them accounting for the new OH-rich intermediate phase and these additional signals.

Firstly, it could be an inevitable phase during dehydroxylation of pyrophyllite forming pyrophyllite dehydroxylate. This process could involve displacements or even migration of Al atoms or distortion of the remaining structure of partially dehydroxylated pyro-
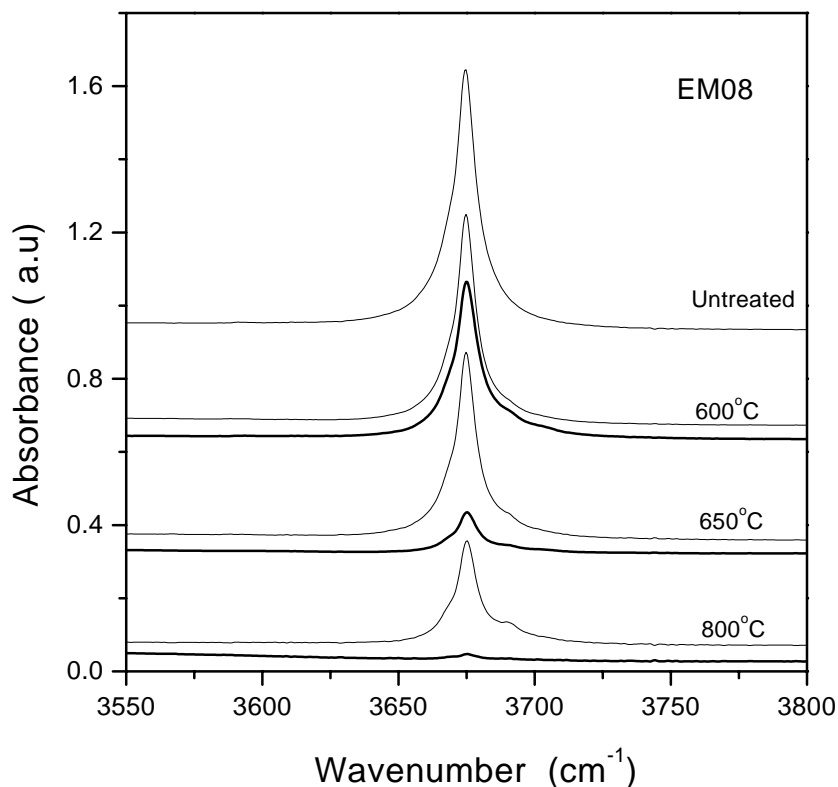
Figure 7. Kinetic effect on the intermediate phase: IR spectra (KBr pellets) in the region $3550-3800$ cm^{-1} of pyrophyllite EM08 samples annealed at 600, 650 and 800°C for 1 h. Thin lines represent $40-60$ mesh samples and thick lines are for 200 mesh samples.

phyllite, resulting in new OH environments as well as possible migration of protons. MacKenzie *et al*. (1985) proposed the formation of an intermediate state containing a five-coordinate Al pair linked by a hydroxyl bridge and an adjacent six-coordinate Al pair, again linked by a hydroxyl group during the dehydroxylation. Guggenheim *et al*. (1987) proposed a model for dehydroxylation of muscovite, and suggested it was also applicable to pyrophyllite and similar dioctahedral 2:1 layer silicates. According to the model of Guggenheim *et al*. (1987), as a result of the loss of some OH groups in partially dehydroxylated samples, sections of the structure contain five-coordinated Al cations and the remaining OH groups become more weakly bound as the Al−OH bonds strengthen. The 'Guggenheim model' predicted that higher energy or temperature would be required to remove those remaining OH species because of their stronger bonding. Fitzgerald *et al*. (1996) suggested that in pyrophyllite dehydroxylate, new, residual, Si−OH−Al sites could be formed based on ^{1}H CRAMPS data from a sample annealed at 550°C for 24 h.

Secondly, it is possible that the phase is formed as a result of potential rehydroxylation of pyrophyllite dehydroxylate at the experimental conditions. Experiments have shown that pyrophyllite dehydroxylate can be rehydroxylated and extra IR signals were observed during rehydroxylation (Heller *et al*., 1962).

Unfortunately, these authors did not give the peak positions of the additional peaks they observed. We digitized their plots and further analysis shows that the peak positions of the extra bands recorded by Heller *et al*. (1962) are consistent with the extra peaks at 3690 and 3702 cm^{-1} observed in this study. This implies that at least the OH-rich intermediate phase can form during rehydroxylation of pyrophyllite dehydroxylate.

Our results show that the dehydroxylation of pyrophyllite is a two-stage process involving the formation of an intermediate phase evidenced by the two additional OH species. However, the two-stage process observed in this study is different from the one proposed by Drits *et al*. (1995) and Muller *et al*. (2000) for the dehydroxylation of aluminous dioctahedral 2:1 layer phyllosilicates. A considerable lengthening of the OH−OH edges in *cis*-vacant 2:1 layers in comparison with the OH−OH edges in the *trans*-vacant is postulated by these authors as the reason for the higher dehydroxylation in minerals consisting of *cis*-vacant 2:1 layers. According to their model, the dehydroxylation of the aluminous *cis*-vacant 2:1 layer occurs in two stages. It involves the replacement of the adjacent OH groups by a residual oxygen atom, the Al cations that originally occupied *cis* and *trans* sites becoming five- and six-coordinated, and transformation into *trans*-vacant dehydroxylated structure by the migration of the Al atoms from former trans-sites to vacant pentagonal prisms. As

a result, the dehydroxylation of aluminous *cis*-vacant 2:1 minerals leads to the same layer structure as that of *trans*-vacant 2:1 layers. It has been recognized that pyrophyllite consists of the *trans*-vacant sites. In pyrophyllite, the dehydroxylation path proposed by Drits *et al*. (1995) (*i.e.* the *cis*-vacant OH-rich phase transforms into a *cis*-vacant OH-poor phase before forming a *trans*-vacant OH-poor dehydroxyl phase) is not expected to take place. Therefore, the model by Drits *et al*. (1995) and Muller *et al*. (2000) implies a single-stage reaction in pyrophyllite. The observation of at least two extra OH species in the intermediate phase during the dehydroxylation of pyrophyllite cannot be simply explained by these authors' models.

In order to understand what happens at the atomic level during the dehydroxylation of pyrophyllite and the nature of the additional OH species, one needs to explain why no extra IR bands have been detected in the frequency region where phonon vibrational modes (*e.g.* Al−O and Si−O stretching and bending) are located. The IR spectra between 350 and 1500 cm^{-1} appear to suggest a simple superposition of two phases (pyrophyllite and pyrophyllite dehydroxylate), and the spectra in this range do not show measurable frequency shifts or the appearance of additional bands, which are generally expected if cation migrations or cation displacements are involved. We also note that the additional OH bands near 3690 and 3702 cm^{-1} can easily form in thick samples and at high temperatures and that the peak positions of these additional OH species are higher than the one at 3675 cm^{-1}, which is difficult to reconcile with them having stronger bonding. Furthermore, we need to understand why they tend to disappear in samples after prolonged annealing, even at 650°C.

Our observations show that the formation of a possible OH-rich intermediate phase depends on annealing temperature, grain-size and annealing time. Short annealing of thick samples at high temperatures could lead to more liberated H$_2$O, and high hydrogen mobility giving new OH sites. This would explain the higher IR intensity for these new OH species which was seen in quenched samples. These new OH species could have a different activation energy for dehydroxylation compared to the original OH species in pyrophyllite, but the difference does not appear significant because the intensity of the signals due to these species also shows the same decrease as the 3675 cm^{-1} signal does during prolonged annealing (Figure 3b) between 650 and 850°C.

One of the important issues of the dehydroxylation of pyrophyllite is to gain an understanding as to what happens to the local structure between 800 and 900°C. On one hand, annealing samples (with grain-size of 40−60 mesh) at 650°C for 5 d leads to loss of 95% OH (Figures 3b and 4), *i.e.* both the OH species giving rise to absorption near 3675 cm^{-1} in pyrophyllite and the additional signals near 3690 and 3702 cm^{-1} all begin to disappear at this temperature. On the other hand, for thick samples (0.30−0.32 mm), these OH species showed no significant decrease in intensity below 750°C, but they suddenly vanish between 850 and 900°C (Figure 5a,b). This difference cannot simply be explained by various OH groups in different environments with different activation energies. We can consider two possible causes. One possibility is that a thermally-induced structural modification occurs which helps to drive the hydrogen species out of pyrophyllite. However, it is puzzling why no extra lines, except those of pyrophyllite and pyrophyllite dehydroxylate, were detected between 350 and 1500 cm^{-1} where Al−O and Si−O vibrations are generally located. Neither did ^{27}Al and ^{29}Si NMR results (Fitzgerald *et al*., 1996) show structural anomalies between 800 and 900°C. The other possible cause is based on our assumption that the process of pyrophyllite dehydroxylation is a combination of dehydroxylation and rehydroxylation. For thick samples, which have a small surface area compared to their volume, H$_2$O formed during dehydroxylation cannot be released quickly, leading to rehydroxylation and the formation of pyrophyllite and the possible OH-rich intermediate phase. At temperatures above 900°C rehydroxylation probably becomes very difficult or the dehydroxylation becomes so fast that the sample could not maintain hydration to the intermediate state. This process does not require the occurrence of any new structure near 900°C. New experiments are underway to check this.

Results of water loss measurements and DTA analysis show that the dehydroxylation of pyrophyllite involves two endothermic processes at 520°C (30% water loss) and at 673°C (60% water loss) (Wardle and Brindley, 1972; MacKenzie *et al*., 1985). Two endothermic peaks of pyrophyllite EM08 at ~650°C (86.7% water loss) and 880°C (13.3% water loss) were observed by DTA-TG with a heating rate of 40°C/min (Wang and Zhang, 1997b). In fact, two endothermic peaks have often been reported for pyrophyllite and their origin has been the subject of some controversy. Based on the discussion above, the appearance of the two extra OH bands at 3690 and 3702 cm^{-1} and the possible OH-rich intermediate phase may contribute to the endothermic peak occurring at the higher temperature. However, the contribution will be affected by kinetic effects. As a result, the temperatures at which a significant loss of water occurs could be changed dramatically by experimental conditions as shown in Figures 3a, 3b, 5a, 5b and 6. The different dehydroxylation temperatures shown by DTA-TG (Wang and Zhang, 1997b) and IR measurements may be due to different thermal conditions (continuous heating in DTA-TG *vs*. isochronal annealing and quenching in IR) and the fact that the dehydroxylation can be affected kinetically. *In situ* IR spectroscopy and ^{1}H NMR may help to gain a better understanding of this issue.

CONCLUSIONS

The IR spectra of pyrophyllite show systematic changes during the dehydroxylation and decomposition processes. Based on IR data, the thermal conversion of pyrophyllite in the temperature range $RT-1500^\circ C$ can be divided into four stages: (1) unchanged state of pyrophyllite ($RT-450^\circ C$); (2) dehydroxylation of pyrophyllite ($500-900^\circ C$); (3) decomposition of pyrophyllite dehydroxylate ($950-1100^\circ C$); (4) formation of cristobalite ($1150-1500^\circ C$).

Thermally-induced dehydroxylation of pyrophyllite to pyrophyllite dehydroxylate leads to a significant structural reorganization. The SiO_4 tetrahedral sheet structure still exists in the pyrophyllite dehydroxylate, but its structure is distorted or subtly changed. The $Si-O-Al$ linkages and the 2:1 structure persist in the pyrophyllite dehydroxylate, but $Si-O-Al$ linkage distances show small changes. Our data do not show clear evidence of the migration of cations.

We have observed, for the first time, spectroscopic evidence of an unknown intermediate state during the dehydroxylation of pyrophyllite. The process of pyrophyllite dehydroxylation is a two-stage reaction, and it involves the appearance of two extra OH bands at 3690 and 3702 cm^{-1} as well as their overtones at 7208 and 7234 cm^{-1}. These bands are observed in the temperature range $500-900^\circ C$ and they show an increase in their intensity with increasing temperature. The appearance of the extra OH species indicates new local structural configurations related to these OH species. This is interpreted as evidence of an unknown intermediate structural state. The existence of the two extra OH species at 3690 and 3702 cm^{-1} may be related to the higher-temperature endothermic peak, and they appear to be similar to bands seen previously in rehydroxylated pyrophyllite.

ACKNOWLEDGMENTS

REFERENCES

Bailey, S.W. (1966) The status of clay mineral structures. *Clays and Clay Minerals*, **14**, 1−23.

Bray, H.J. and Redfern, S.A.T. (2000) Influence of counterion species on the dehydroxylation of Ca^{2+}-, Mg^{2+}-, Na$^+$- and K$^+$-exchanged Wyoming montmorillonite. *Mineralogical Magazine,* **64**, 337−346.

Bray, H.J., Redfern, S.A.T. and Clark, S.M. (1998) Time-temperature-dependent dehydration of Ca-montmorillonite: an *in situ* X-ray diffraction study. *Mineralogical Magazine*, **62**, 647−656.

Brindley, G.W. and Wardle, R. (1970) Monoclinic and triclinic forms of pyrophyllite and pyrophyllite anhydride. *American Mineralogist,* **55**, 1259−1271.

Drits, V.A., Besson, G. and Muller, F. (1995) An improved model for structural transformations of heat-treated aluminous dioctahedral 2:1 layer silicates. *Clays and Clay Minerals*, **43**, 718−731.

Eberl, D.D. (1979) Synthesis of pyrophyllite polytypes and mixed layers. *American Mineralogist,* **64**, 1091−1096.

Farmer, V.C. (1974) *The layer silicates.* Pp. 331−363 in: *The Infrared Spectra of Minerals* (V.C. Farmer, editor). Monograph, **4**. Mineralogical Society, London.

Fitzgerald, J.J., Dec, S.F. and Hamza, A.I. (1989) Observation of five-coordinated Al in prophyllite dehydroxylate by solid-state ^{27}Al NMR spectroscopy at 14 T. *American Mineralogist,* **74**, 1405−1408.

Fitzgerald, J.J., Hamza, A.I., Dec, S.F. and Bronnimann, C.E. (1996) Solid-state ^{27}Al and ^{29}Si NMR and ^{1}H CRAMPS studies of the 2:1 phyllosilicate pyrophyllite. *Journal of Physical Chemistry*, **100**, 17351−17360.

Frost, R.L. and Barron, P.F. (1984) Solid-state silicon-29 and aluminium-27 nuclear magnetic resonance investigation of the dehydroxylation of pyrophyllite. *Journal of Physical Chemistry*, **88**, 6206−6209.

Guggenheim, S., Chang, Y.H. and Koster van Groos, A.F. (1987) Muscovite dehydroxylation: High-temperature studies. *American Mineralogist*, **72**, 537−550.

Heller, L. (1962) The thermal transformation of pyrophyllite to mullite. *American Mineralogist,* **47**, 156−157.

Heller, L., Farmer, V.C., Mackenzie, R.C., Mitchell, B.D. and Taylor, H.F.W. (1962) The dehydroxylation and rehydroxylation of triphormic dioctahedral clay minerals. *Clay Minerals Bulletin*, **5**, 56−72.

Ishii, M., Shimanouchi, T. and Nakahirea, M. (1967) Far infrared absorption spectra of layer silicates. *Inorganica Chimica Acta,* **1**, 387−392.

Kloprogge, J.T. and Frost, R.L. (1999) An infrared emission spectroscopic study of synthetic and natural pyrophyllite. *Neues Jahrbuch für Mineralogie, Monatshefte*, 62−74.

Lee, J.H. and Guggenheim, S. (1981) Single crystal X- ray refinement of pyrophyllite − 1*Tc*. *American Mineralogist,* **66**, 350−357.

MacKenzie, K.J.D., Brown, I.W.M., Meinhold, R.H. and Bowden, M.E.J. (1985) Thermal reactions of pyrophyllite studied by high-resolution solid-state ^{27}Al and ^{29}Si nuclear magnetic resonance spectroscopy. *Journal of the American Ceramic Society*, **68**, 266−272.

Muller, F., Drits, V., Plançon, A. and Robert, J.L. (2000) Structural transformation of 2:1 dioctahedral layer silicates during dehydroxylation-rehydroxylation reactions. *Clays and Clay Minerals*, **48**, 572−585.

Rayner, J.H. and Brown, G. (1966) Structure of pyrophyllite. *Clays and Clay Minerals*, **25**, 73−84.

Russell, J.D., Farmer, V.C. and Velde, B. (1970) Replacement of OH by OD in layer silicates, and identification of the vibrations of these groups in infrared spectra. *Mineralogical Magazine*, **37**, 869−879.

Stubican, V. and Roy, R. (1961) Proton retention in heated 1:1 clays studied by infrared spectroscopy, weight loss deuterium uptake. *Journal of Physical Chemistry*, **65**, 1348−1351.

Van der Marel, H.T. and Beutelspacher, H. (1976) *Atlas of Infrared Spectroscopy of Clay Minerals and their Admixtures.* Elsevier, Amsterdam, 396 pp.

Wang, L. (1994) Metallogeny of pyrophyllite in the coastal region of Southeast China and pyrophyllite's thermal stability. Ph.D. thesis, Changsha Institute of Geotectonics, Chinese Academy of Sciences (in Chinese).

Wang, L. and Zhang, Z.Y. (1997a) High-temperature phases of pyrophyllite and their evolutionary characteristics. *Chinese*

Science Bulletin, **42**, 140−143.

Wang, L. and Zhang, Z.Y. (1997b) Principles and methods of quantitative analysis on *b*-axis disorder in 2:1 dioctahedral phyllosilicate. *Chinese Science Bulletin*, **42**, 1980−1992.

Wardle, R. and Brindley, G.W. (1971) The dependence of the wavelength of AlK$_\alpha$ radiation from alumino-silicates on the Al−O distance. *American Mineralogist,* **56**, 2123−2128.

Wardle, R. and Brindley, G.W. (1972) The crystal structures of pyrophyllite, 1*Tc*, and of its dehydroxylate. *American Mineralogist,* **57**, 732−750.

Wen, L., Liang, W.X., Zhang, Z.G. and Huang, J.C. (1988) *The*

Infrared Spectroscopy of Minerals. Chongqing University Press, Chongqing, China, 190 pp. (in Chinese).

Yang, Y.X., Zhang, N.X. and Su, S.B. *et al.* (1994) *Clay Minerals of China*. Geological Publishing House, Beijing, 297 pp. (in Chinese).

Zhang, M., Wruck, B., Graeme-Barber, A., Salje, E.K.H. and Carpenter, M.A. (1996) Phonon-spectroscopy on alkali-feldspars: phase transitions and solid solutions. *American Mineralogist,* **81**, 92−104.